NTU Journal for Renewable Energy (2023) Vol. 5 (1): 61-73
DOI: https://doi.org/10.56286/ntujre.v4i1

IRAQI Academic Scientific Journals

EISSN: 2788-9920
NTU Journal for Renewable Energy
Available online at:
https://journals.ntu.edu.iq/index.php/NTU-JRE

Load Frequency Control With Renewable Energy Sources Using Practical Swarm Optimization Based On PID

Nagham Hikmat Aziz[1]

[1]Electrical Engineering Department, Collage of Engineering, University of Mosul.

Article Informations

Received: 10 – 06 - 2023
Accepted: 07 – 08 - 2023
Published: 28 – 08- 2023

Corresponding Author:
Nagham Hikmat Aziz

Email:
naghamhikmat@uomosul.edu.iq

Key words:
Renewable generation sources, hybrid generating systems, PSO controller, LFC.

ABSTRACT

Future competitive solutions for the production of electricity may be provided by emerging renewable energy sources (RESs) technologies as wind, solar photovoltaic, and solar thermal power systems. In this study, simulation tests have been conducted on autonomous hybrid generating systems(HGSs) made up of diesel engine generators (Degs), fuel cells (FCs), wind turbine generators (Wpg), solar photovoltaic generators (Pvpg), battery energy storage systems (Bess), and flywheels (Fess). The abrupt fluctuations in load, generation, or both cause the power system's frequency to vary. PID controller tuning using particle swarm optimization (PSO) is used for the optimization of controllers' gains of the proposed hybrid systems. The proposed method is compared with a genetic algorithm (GA) and a traditional PID controller. To test the proposed controller, three different scenarios were used: first, changing the load's value with a fixed value over a set period of time; second, changing the load's value with variable values; and third, changing the load's value with a variable value while changing the system parameters. the simulation results reveal that the suggested controller performs better and is more resilient against load and generational disruptions by reducing the maximum overshoot value and settling time by 70% and 65%, respectively, and by 14.2% and 5% when compared to a GA-PID control.

1. Introduction

Recently, the need to use renewable energy sources (RESs) has increased due to the high increase in population in all countries of the world. RES such as solar energy and wind energy are used as a source of generation in remote areas where there are no main grid stations, and thus we get a solution to the problem of fossil fuel depletion from using the HGSs [1]. RESs and traditional generation sources, in addition to energy storage devices(ESDs), are what is called a microgrid, which is used to ensure the continuity of service supply over time [2].

Among the advantages of using the HGSs is the promotion of renewable resources when a sudden event occurs in the movement of wind and its speed, the change in the intensity of solar radiation, the reduction of energy costs, as well as the reduction of unwanted gas emissions[3].

One of the fundamental and significant issues with the power system (PS) is controlling the load frequency. When load disruptions occur, the active power supplied by the generation sources helps to keep the system frequency within acceptable bounds[4].

Inequality in power generation and consumption is caused by unpredictably changing total energy demand. A departure from the desired frequency value hurts the quality of the electricity generated. The frequency deviation from its nominal value should be kept to a minimum and within allowable bounds for efficient electric power consumption and functioning of frequency dependent equipment. To complement the synchronous machine's governor and eliminate the frequency and net tie-line interchange deviations, load frequency control (LFC) is introduced to the system.[4]

There are various methods for controlling the frequency of the load, such as the conventional PID controller, which is regarded as the simplest and most straightforward controller in the power system, but one of its disadvantages is the selection of the values of the gain, so some modern techniques are used. The researchers in [5] used the GA method to select the optimal values for the controller PID values and compare them with the conventional PID and fuzzy logic (FL) for a two-area system. Ref [6] provides a review on controlling LFC using a PID controller. To adjust the gain values of the PID controllers, the researchers in [7] employed the Bacterial Foraging Optimization technique. In a MATLAB/SIMULINK model created as part of the LFC study for HGSs, it is shown that the BFO-adjusted PID controllers can maintain rated frequency under the variation of LD and variable generation from wind/PV sources. The researchers in [8] designed a LFC for a multi-zone PS using an extreme population algorithm considering the load dynamics. Ref [9] used BESS battery energy storage in a DC Micro-grid to control the frequency in case a diesel generator and its governor fails to operate. The researchers in [10] used a meta-heuristic hybrid algorithm to improve the dynamic stability of a multi-area containing RESs system by studying the effect of MG penetration for multiple operating states. Relying on an IEEE-39 conveyor system with a wind station, the researchers were

able to optimize Jaya modified for LFC over the Internet [11].

In order to manage the load frequency in a microgrid, this research uses an optimal technique. The constant parameters of the traditional PID controller have been overcome in the suggested solution by a practical swarm optimization. The PSO tuning PID controller, utilized in this method, solves the PID problem and can support uncertainties brought by changes in operational circumstances, system modeling, parametric modifications, and other factors. It also delivers desired performance. The findings show that PID-PSO is more resilient than PID-GA controller and PIDc.

2. Hybrid Power System

Recently, the addition of RESs , whose nature depends on environmental conditions, has spread to the power system, causing disturbances that affect the stability of the network. This occurs as a result of the system's reliance on small-capacity, low-inertial-moment generating units. In situations when the input is stochastic (wind or solar) or there are outages in the generating units, this leads to extreme swings in system parameters like frequency and voltage. Therefore, it might be important for RESs to both produce electricity and take part in frequency management.

The HGSs consist of Pvpg, Wpg, FCs, Degs, Bess, and Fess [12]. Figure .1 shows a complete diagram of the HGSs with a proportional-integral-derivative controller (PIDc). The transfer function and the state-state variable are considered the basis on which to design the control unit and represent the power system and convert it into a mathematical model with some assumptions[13]. The transfer function of all the parts of the system is represented below:Wind power generator transfer function:

$$\mathrm{GWpg} = \frac{\mathrm{KWpg}}{1+s.\mathrm{TWpg}} \qquad (1)$$

where KWpg and TWpg represented the gain of Wpg and time constant of Wpg respectively .

1- Photovoltaic power Generation:

$$\mathrm{GPv} = \frac{\mathrm{KPvpg}}{1+s.\mathrm{TPvpg}} \qquad (2)$$

where KPvpg and TPvpg represented the gain of Pvpg and time constant of Pvpg respectively.

2- FCs system :

$$\mathrm{GFCs} = \frac{\mathrm{KFCs}}{1+s.\mathrm{TFCs}} \qquad (3)$$

where KFCs and TFCs represented the gain of FCs and time constant of FCs respectively.

3- Diesel Engine Generators :

$$\mathrm{GDegs} = \frac{\mathrm{KDegs}}{1+s.\mathrm{TDegs}} \qquad (4)$$

where KDegs and TDegs represented the gain of Deg and time constant of Deg respectively.

4- Single area system:

$$\mathrm{Gsystem} = \frac{1}{\mathrm{D}+s.\mathrm{M}} \qquad (5)$$

5- Energy Storage Systems:

$$\mathrm{GBess} = \frac{\mathrm{KBess}}{1+s.\mathrm{TBess}} \qquad (6)$$

$$\mathrm{GFess} = \frac{\mathrm{KFess}}{1+s.\mathrm{TFess}} \qquad (7)$$

where KBess, KFess , TFess and TBess represented the gain of Bess , gain of Fess , time constant of Bess and time constant of Fess respectively [13].

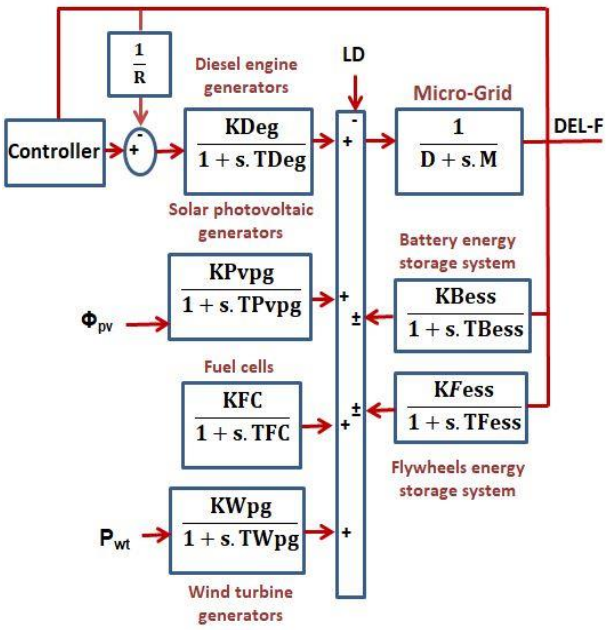

Figure .1 Block diagram of HGSs model

3. The Paradigm of The Generated Power and Load

Equation.8 expresses the changes, which are by nature small and random, in addition to the critical deviation for Wpg, Pvpg and power load demand (PLD).

$$P = \left(\frac{\varphi * \eta * \sqrt{\beta} * \left(1 - G(s)\right) + \beta}{\beta}\right) * \Gamma \qquad (8)$$

P stands for the generated power of Pvpg or Wpg and load, φ denotes the power's stochastic value, β denotes its average value, and η is a constant that normalizes the generated or demanded powers and Γ It is a signal with gain dependent on the time that causes a surprising change in the average random power value [14]. Figure. 2 shows the simulation of solar or wind power generation and load based on the Equation. 8

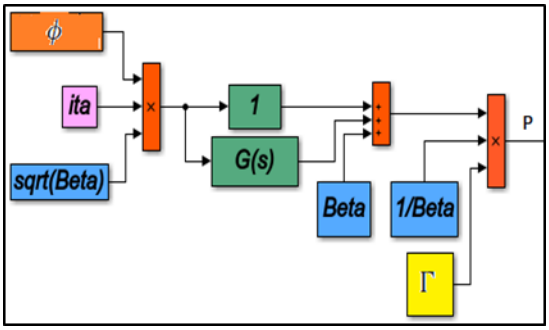

Figure .2 Generated power of solar or wind and load**.**

The φ is obtained using a low-pass filter with a white noise block to randomly obtain a variable wind, solar , load power. Values of parameters for Wpg are: $\varphi \sim U\,(-1,1)$, η= 0.8, β =10, $G(s) = 1/(10^4 s + 1)$, Γ=0.28u (t) (9)

u (t) is the step function.
Values of parameters for Pvgp are: $\varphi \sim U\,(-1,1)$, η= 0.1, β =10, $G(s) = 1/(10^4 s + 1)$,
Γ= 0.07 u (t) (10)

Values of parameters for PLD are: $\varphi \sim U\,(-1,1)$, η= 0.9, β =10,
$G(s) = 300/(300s + 1) + 1/(1800s + 1)$,

$$\Gamma = \begin{bmatrix} 0.9\,u\,(t) + 0.03u\,(t - 110) \\ 0.15\,u\,(t - 130) + -0.2u\,(t - 150) \\ -0.15\,u\,(t - 170) + 0.2u\,(t - 190) \end{bmatrix} \qquad (11)$$

The equation of the transfer PIDc performed as the following :

$$G_{PID} = K_P + \frac{K_I}{s} + K_D.s \qquad (12)$$

The form of PIDc is depicted in figure.3, and K_P stands for the proportional gain, K_I for the integral gain, and K_D for the derivative gain [15].

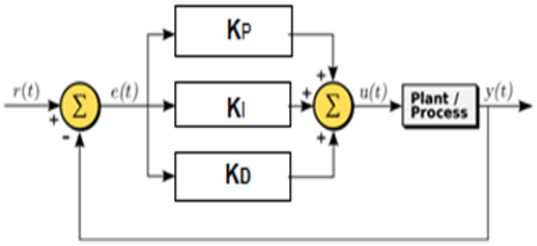

Figure .3 Form of the PIDc

Using the PSO technique to adjust the values of the PIDc parameters and choose the optimal values for them to control the frequency deviation (DEL_F). The controller's parameters were chosen using the objective integrated time absolute error (ITAE) function.

$$ITAE = \int_0^{tsim} tsim * |e(t)|dt \qquad (13)$$

Where *e(t)* represents the (DEL_F) of the hybrid system and *tsim* equal the simulation time.

4- Practical Swarm Optimization

The practical swarm optimization algorithm (PSOa) was developed by Eberhart and Kennedy in 1995, and it simulates the social behavior of flocks of birds and fish that these flocks use to find shelter, food sources, or another suitable habitat for them. This algorithm is one of the best-approved algorithms for solving many technologies. The basic principles of the collective behavior of birds represent search in the search space (D-dimension). Its algorithm is characterized by the following:

•Homogeneity: All birds have the same pattern of behavior, and the flock moves without a leader.
• Locality: the movement of each bird will be affected only by the movement of neighboring birds, and vision is the most important sense of the bird to organize the flock.
•Avoidance Collision: The bird avoids its mates in the flock.
•Centering Flock: The bird tries to stay close to its mates in the flock.
• Matching Velocity in the squadron
•The bird tries to match the speed of its mates.

Steps to technique PSO:
1- Initialize the velocities and locations with initial values, where the velocity values are zero at the beginning.
2- Computation of the fitness function (Fit_F) for the values for each individual representing Pbest (a personal best site) in an elementary way.
3- Calculating the value of Gbest (a general best location), comparing the value of the Fit_F with the best location in the flock as a whole. If the current value is better than Gbest, then the value of Gbest is set equal to the current location.
4- Updating the velocity and location of each individual in the squadron at cycle Itr=1, based on the two equations

$$v_i^{k+1} = w^k v_i^k + c_1 r_1^k \left(Pbest_i^k - s_i^k\right) + c_2 r_2^k \left(Gbest^k - s_i^k\right) \qquad (14)$$

$$s_i^{k+1} = s_i^k + v_i^{k+1} \quad (15)$$

Since w represents the weight of inertia, c1 and c2 are positive constants called learning factors, r1 and r2 are two random numbers within the range [0,1] n, i=1,2,……,n, equal to the size of the swarm, k=1,2 represents the Iteration.

5- Calculating the Fit_F for the values for each individual for the new values.

6- Comparing the value of the Fit_F for each individual with its Pbest. If the new value is better than the Pbest, then it is placed for the new location in the problem space.

7-The steps from the second step are repeated according to the cycles, in the end we get the value of gbest. Figure .4 show the flowchart of the PSOa control .

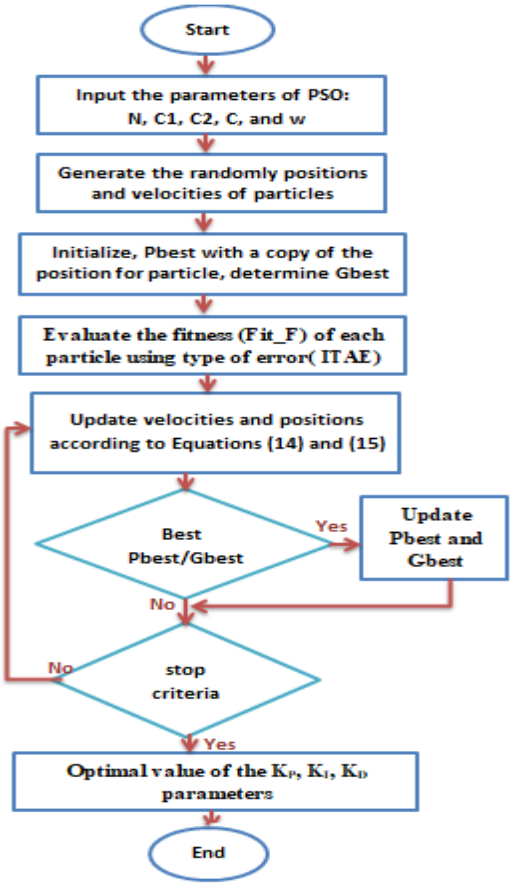

Figure .4 Flowchart of PSOa control

5- Simulation Result

Using Matlab 2020, the model under study is represented HGSs that contain a group of RESs with some ESDs. The abrupt shift in generation and load has an impact on the frequency and power stability, and the controller works to mitigate this effect by sending feedback signals to secondary sources such as the FC and DEG and storage devices. as shown in the figure.5. The D, M, and R parameters in the microgrid are equal to 0.0015 (pu/Hz), 0.1667, and 3 respectively, and all values of parameters of the model in Appendix A.

Genetic algorithm (GA) is one of the optimization techniques, the working steps of this technique with the diagram in [17]. This technique was applied to find the optimal gains for PIDc. Using optimtool Toolbox in MATLAB, and compered with the proposed PSOa to control the DEL_F .

ITAE was applied to PSOa and GA to optimize for Kp, Ki, and Kd. All Inputs and parameter values for PSOa and GA are in Table (1), and figure.6 and 7 show the fast converging behavior for the Fit_F value plotted against generation of PID controller vs iteration for PSOa and GA techniques with the upper limit of iterations set 100 and 50, respectively. It can see from the figure that more than 40 iterations are required to reach the best Fit_F of value 2.18 for PSOa and almost three iterations for GA of value 2.53963.

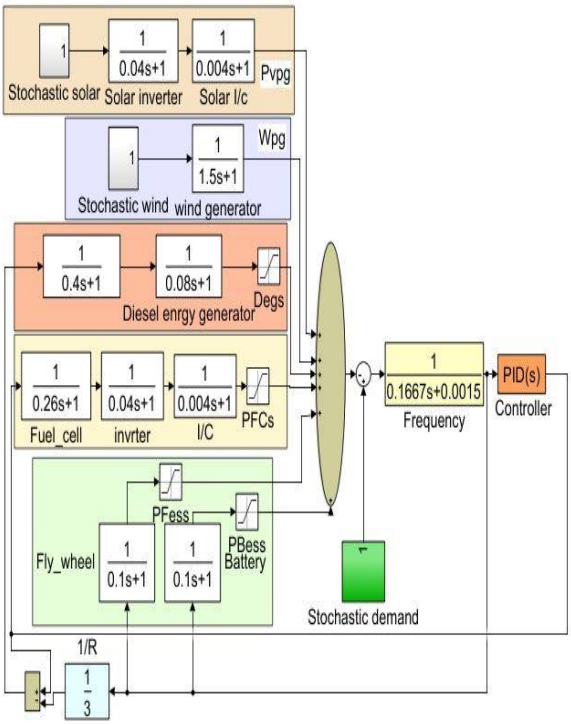

Figure .5 HGSs model in MATLAB.

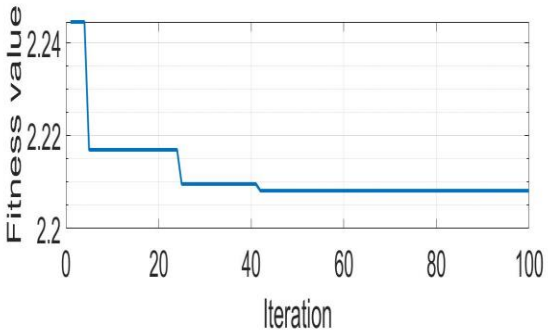

Figure .6 Fit_F value plotted against generation in PSOa.

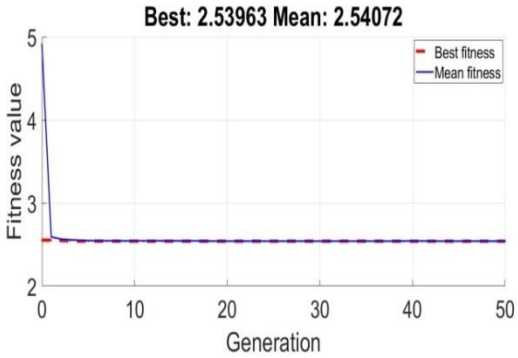

Figure.7 Fit_F value plotted against generation in GA.

Table.1 Inputs and parameters PSOc and GA algorithm

	Parameters	Values
PSO	PSO Iteration No.	100
	Swarm size	15
	Max Weight (w)	0.9
	Min Weight (w)	0.2
	Personal iterations	1.0
	Inertia Coefficient (C1)	0.2
	Inertia Coefficient (C2)	0.5
	PSO Iteration No.	100
	Swarm size	15
GA	Number of variables	3
	Population size	Default
	Creation function	Uniform
	Selection function	Tournament
	Crossover fraction	Default
	Crossover function	Arithmetic
	Fitness function	ITAE
	Stopping criteria	Default

Table 2 displays the optimization findings for the PSO-PID, GA-PID, and PIDc gains, and Figure 8 displays the DEL-F PIDc, GA-

PID, and PSO-PID controllers. Figure 8 clearly shows that the suggested PSO-PID controller case, followed by the GA-PID controller case, then PIDc case, had the lowest peak value overshoot for the response DEL-F after simulation in 200 sec with the values (0.07902, 0.09212, 0.2634) and the lowest settling time value (0.332, 0.35, 0.95) seconds. That is, the peak overshoot value of the response and the holding time of the PSO-PID controller decreased by 70% and 65% compared to the conventional PIDc controller, and by 14.2% and 5% compared to the GA-PID controller, respectively.

Table.2 PID ,GA-PID and PSO-PID gain parameters with using ITAE objective function

PID gain parameters	**ITAE**		
	Kp	Ki	Kd
PIDc	4.23	20.67	0.743
GA_PID	13.2	52.12	2.138
PSO_PID	7.43	42.41	2.43

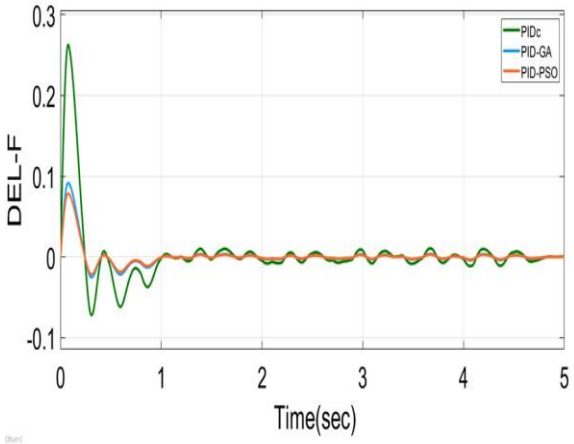

Figure 8. DEL-F for PIDc ,GA-PID and PSO-PID controllers

Three instances were examined to analyze the simulation results in order to verify the system's dynamic performance:

1- **Control the system frequency value by changing the load with a fixed value.**

In this part, load step variations of 0.01 are taken into account. Additionally, simulation outcomes for the LFC for load variations of 0.01 steps are shown in Fig. 9. Fig. 10 depicts the power output of solar panels, and wind turbines. Fig. 11 also displays the power of Deg output. Figure 12 depicts a DEL-F for simulating the duration from 100 to 200 seconds. With a focus on adding the load at the time of 130 seconds, which is comparable to all other situations of adding the load 0.01 p.u at other times. The frequency response of the suggested method for LFC is better, faster, and with fewer oscillations than other methods, according to the results.

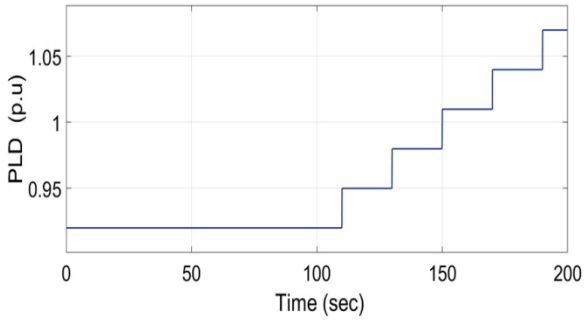

Figure 9. LD power step variation 0.01 p.u

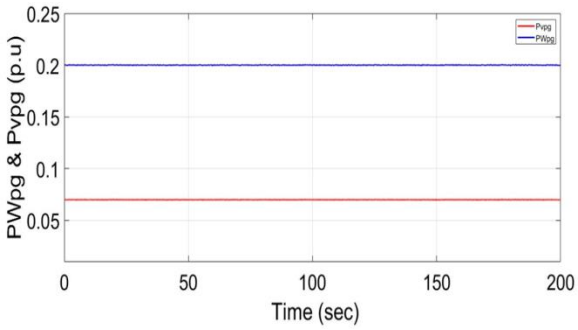

Figure 10. PWpg & Pvpg output power in p.u .

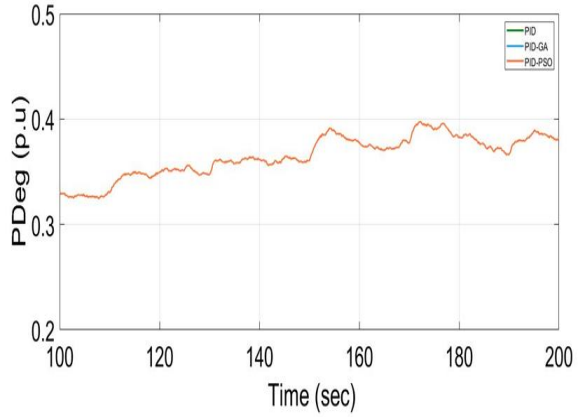

Figure 11. PDeg output power in p.u in step load variation 0.01 p.u.

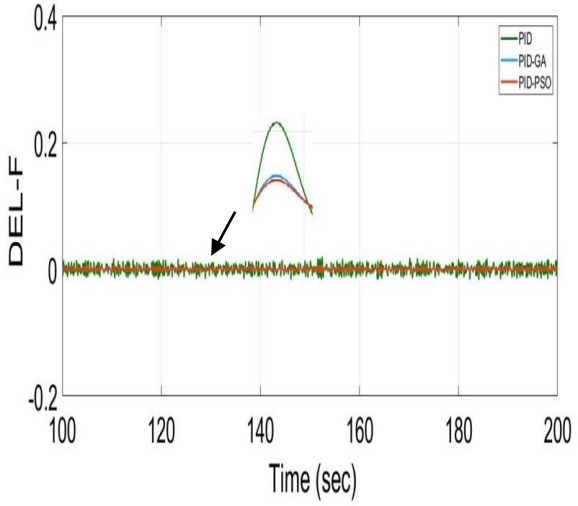

Figure 12. DEL-F for in step load variation 0.01 p.u .

2- Control the system frequency value by changing the load with a variable value.

In this part, step load changes are introduced to the microgrid to demonstrate the proposed controller's robustness against various load changes at various times. Fig. 13 depicts these changes in load. The optimization outcomes of the parameters match those of Table 2's parameters. Fig. 14 depicts the simulation results of the microgrid's frequency response in conjunction with varying load changes. Additionally, Figure 15, 16, and figure. 17 display the generation capacity of Deg , FC with Bess & Fess respectively. Figure 14 illustrates how the proposed controller, which has the ability to lessen DEL-F brought on compares favorably to earlier controllers in terms of response speed, high damping, and less amplitude. The GA controller unit comes next, which performs well in decreasing DEL-F when compared to PIDc.

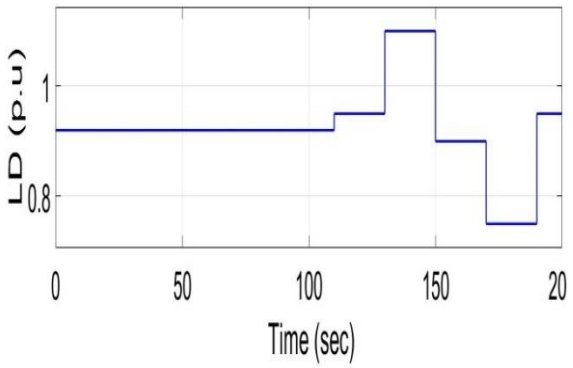

Fig. 13 shows the microgrid's variable step load adjustments

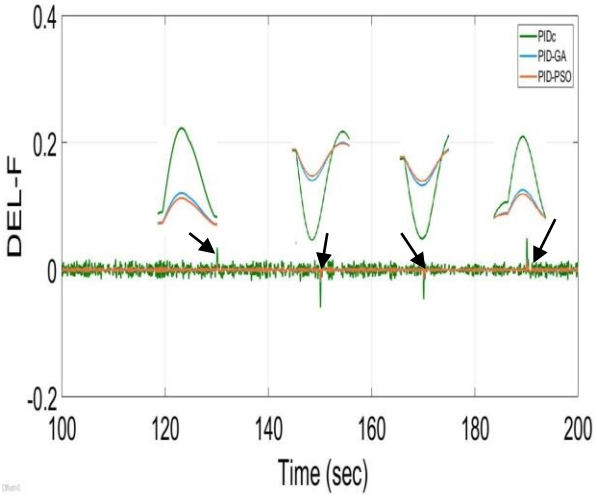

Figure 14 shows the DEL-F to variations in the variable step load that were obtained for various control strategies.

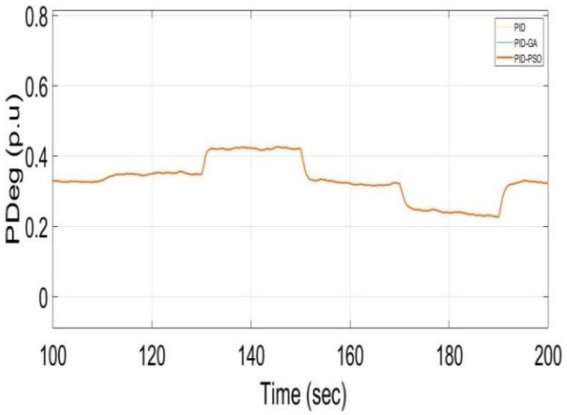

Figure 15. Output power in p.u. of the PDeg under various load situations

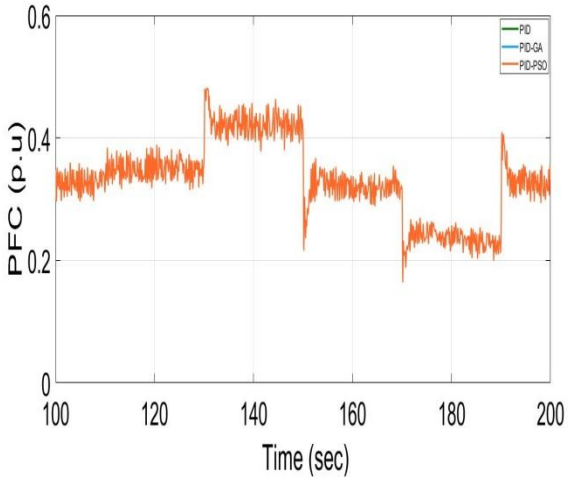

Figure 16. Output power in p.u. of the PFCs under various load situations

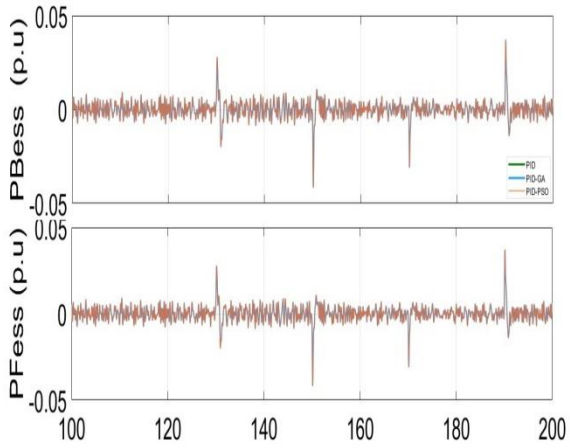

Figure 17 shows the significant rate-constrained nonlinear behavior of the energy storage devices.

3- Control the system frequency value by changing the load with a variable value while changing the system parameters.

In this part, the microgrid has undergone many changes to the system parameters by increasing the H value and TDeg by 30%, the R-value by 15%, and decreasing the D value by 25% in order to illustrate the adaptability of the suggested controller to these changes. In addition, the chosen load type takes the shape of a time-varying step in accordance with the scenario shown in Fig. 13. Fig. 18 depicts the simulation results of the DEL-F with regard to changes in system parameters. Additionally, Figure 19, 20, and figure. 21 display the generation capacity of Deg , FC with Bess & Fess respectively.

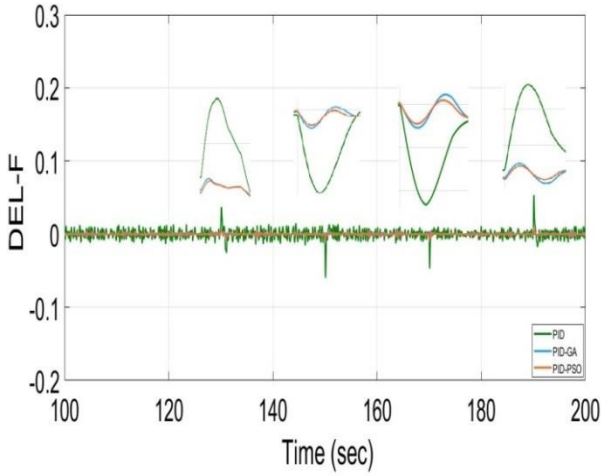

Figure 18 Shows the DEL-F response for changing the system parameters with variable value of load.

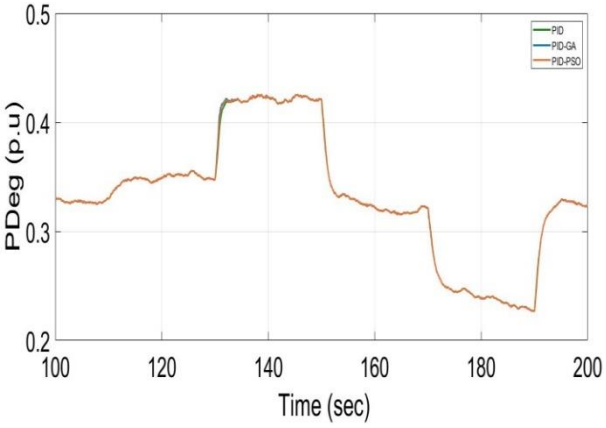

Figure 19. Output power in p.u. of the PDegs under changing the system parameters with variable value of load.

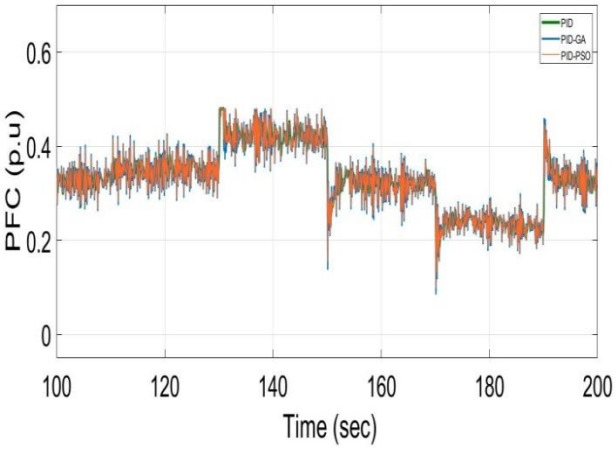

Figure 20. Output power in p.u. of the PFCs under changing the system parameters with variable value of load.

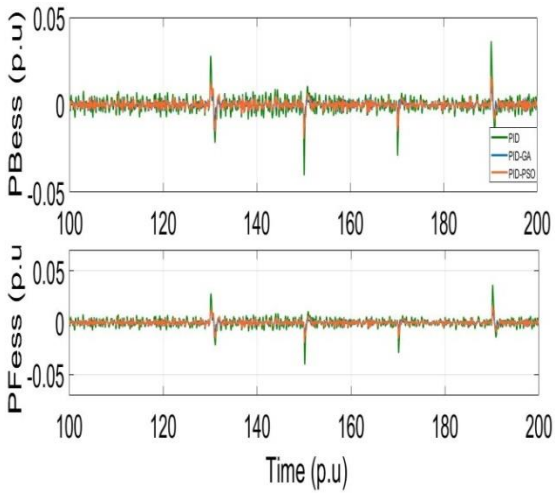

Figure 21 shows the significant rate-constrained nonlinear behavior of the energy storage devices.

Conclusion

This study examines the LFC of an isolated microgrid made up of FC, Wtg, Pv system, Bess, and Fess. PID controllers coupled in the feedback of energy storage devices BESS and FESS as well as conventional sources like DEG and FC are used to control the frequency. By minimizing an objective function (ITAE), the Particle Swarm Optimization Algorithm and Genetic Algorithm are used to optimize the PID controller parameters. The results obtained showed that the performance of the PID-PSO approach decreased the maximum overshoot value and settling time by 70% and 65% compared to the conventional PIDc controller, and by 14.2% and 5% compared to the GA-PID control. This proves that the performance of PID-PSO is better than that of PID-GA.

Appendix A:

Parameters of the HGSs Component

Parameters	Gain	Time constant (s)
Wtg	KWpg=1	TWpg=1.5
Pvpg	KPvpg=1	TPvpg=1.8
FCs	KFc=0.01	TFc=4
Degs	KDeg=0.003	TDeg=2
Bess	KBess=−0.003	TBess=0.1
Fess	KFess=−0.01	TFess=0.1

References

[1] R. M. Sidi Brahim, H. M'hamed, R. Taleb, and A. LEMRABOUT, "Load Frequency Control of Hybrid power System using Classical PID Controller", Computer and Engineering, vol. 1, Issue: 1, Dec. 2020.

[2] Regad Mohamed Sidi Brahim, M'hamed Helaimi, Rachid Taleb "Control of isolated microgrid based renewable energy generation using PID controller" , International Journal of Applied Power Engineering (IJAPE), vol. 10, Issue: 2, June 2021, pp. 127~134, DOI: 10.11591/ijape.v10.i2.pp127-134.

[3] H. A. Kazem, H. A. S. Al-Badi, A. S. Al Busaidi and M. T. Chaichan, "Optimum design and evaluation of hybrid solar/wind/diesel power system for Masirah Island," Environment, Development and Sustainability, vol. 19, pp. 1761-1778, 2017.

[4] Fan, Wei, Zhijian Hu, and Veerapandiyan Veerasamy, "PSO-Based Model Predictive Control for Load Frequency Regulation with Wind Turbines" Energies, vol. 15, Issue: 21 ,2022 https://doi.org/10.3390/en15218219.

[5] E.Cam, G. Gorel, H. Mamur. Use of the Genetic Algorithm-Based Fuzzy Logic Controller for Load-Frequency Control in a Two Area Interconnected Power System. Applied Sciences, vol. 7,Issue: 3, pp. 308 ,2017, https://doi.org/10.3390/app7030308.

[6] Yogesh V. Hote, and Shivam, "PID Controller Design for load frequency control: Past, Present and future challenges", IFAC PapersOnLine, vol. 51, Issue: 48, pp.604-609,2018, https://doi.org/10.1016/j.ifacol.2018.06.162.

[7] I. Koley, P. S. Bhowmik and A. Datta, "Load frequency control in a hybrid thermal-wind-photovoltaic power generation system," 2017 4th International Conference on Power, Control & Embedded Systems (ICPCES), Allahabad, India, 2017, pp. 1-5,doi:10.1109/ICPCES.2017.8117656.

[8] Min-Rong Chen, Guo-Qiang Zeng, Xiao-Qing Xie, "Population extremal optimization-based extended distributed model predictive load frequency control of multi-area interconnected power systems", Journal of the Franklin Institute vol. 355, Issue: 17 pp.8266–8295,2018,https://doi.org/10.1016/j.jfranklin.2018.08.020.

[9] S. S. Puhan, R. Sharma and S. R. Lenka, "Frequency control through BESS and SOFC based fuel cell in a Multi source Microgrid," 2021 1st Odisha International Conference on Electrical Power

Engineering, Communication and Computing Technology(ODICON), Bhubaneswar, India, 2021, pp. 1-6, doi: 10.1109/ODICON50556.2021.9428931.

[10] K. H. Abdulkhader, J. Jacob and A. Mathew, "Robust type-2 fuzzy fractional order PID controller for dynamic stability enhancement of power system having RES based microgrid penetration," Int. Journal of Electrical Power & Energy Systems, vol. 110, pp. 357–371, 2019.

[11] Chittaranjan Pradhan, Chandrashekhar N. Bhende, "Online load frequency control in wind integrated power systems using modified Jaya optimization", Engineering Applications of Artificial Intelligence vol.77,pp. 212–228, 2019. https://doi.org/10.1016/j.engappai.2018.10.003.

[12] Regad, Mohamed, M'hamed Helaimi, Rachid Taleb, Ahmed M. Othman, and Hossam A. Gabbar. "Frequency control of microgrid with renewable generation using PID controller based krill herd." Indonesian Journal of Electrical Engineering and Informatics (IJEEI),vol. 8, Issue: 1, pp. 21-32 , 2020.

[13] Yang-Wu, S., Xun, M., Ao, P., Yang-Guang, W., Ting, C., Ding, W., et al. "Load Frequency Control Strategy for Wind Power Grid-Connected Power Systems Considering Wind Power Forecast," in 2019 IEEE 3rd Conference on Energy Internet and Energy System Integration (EI2) ,Changsha, China, 2019. doi:10.1109/EI247390. 2019.9062084.

[14] I. Pan and S. Das, "Kriging Based Surrogate Modeling for Fractional Order Control of Microgrids," in IEEE Transactions on Smart Grid, vol. 6, Issue: 1, pp. 36-44, Jan. 2015, doi: 10.1109/TSG.2014.2336771.

[15] Z. Zhou, G. M. Huang and S. P. Bhattacharyya, "Modern PID controller design for load frequency control," 2016 North American Power Symposium (NAPS), Denver, CO, USA, 2016, pp. 1-6, doi: 10.1109/NAPS.2016.7747947.

[16] Mohamed, T., Abubakr, H., Hussein, M., Shabib, G. "Load Frequency Controller Based on Particle Swarm Optimization for Isolated Microgird System", International Journal of Applied Energy Systems, vol. 1, Issue: 2, pp. 69-75, 2019. doi: 10.21608/ijaes.2019.169953.

[17] Tianyu Hui, Wenjie Zeng, Tao Yu, "Core power control of the ADS based on genetic algorithm tuning PID controller", Nuclear Engineering and Design,vol. 370,pp.110835,2020,https://doi.org/10.1016/j.nucengdes.2020.110835.